

Viral Dynamics during Structured Treatment Interruptions of Chronic Human Immunodeficiency Virus Type 1 Infection

Simon D. W. Frost,^{1,*} Javier Martinez-Picado,² Lidia Ruiz,² Bonaventura Clotet,²
and Andrew J. Leigh Brown^{1,3}

Department of Pathology, University of California, San Diego, California¹; IrsiCaixa Foundation, Hospital Universitari Germans Trias i Pujol, Badalona, Spain²; and Centre for HIV Research, University of Edinburgh, Edinburgh, Scotland³

Received 14 June 2001/Accepted 29 October 2001

Although antiviral agents which block human immunodeficiency virus (HIV) replication can result in long-term suppression of viral loads to undetectable levels in plasma, long-term therapy fails to eradicate virus, which generally rebounds after a single treatment interruption. Multiple structured treatment interruptions (STIs) have been suggested as a possible strategy that may boost HIV-specific immune responses and control viral replication. We analyze viral dynamics during four consecutive STI cycles in 12 chronically infected patients with a history (>2 years) of viral suppression under highly active antiretroviral therapy. We fitted a simple model of viral rebound to the viral load data from each patient by using a novel statistical approach that allows us to overcome problems of estimating viral dynamics parameters when there are many viral load measurements below the limit of detection. There is an approximate halving of the average viral growth rate between the first and fourth STI cycles, yet the average time between treatment interruption and detection of viral loads in the plasma is approximately the same in the first and fourth interruptions. We hypothesize that reseeding of viral reservoirs during treatment interruptions can account for this discrepancy, although factors such as stochastic effects and the strength of HIV-specific immune responses may also affect the time to viral rebound. We also demonstrate spontaneous drops in viral load in later STIs, which reflect fluctuations in the rates of viral production and/or clearance that may be caused by a complex interaction between virus and target cells and/or immune responses.

Treatment of chronic human immunodeficiency virus type 1 (HIV-1) infection with antiretroviral agents can be effective in suppressing viral loads in the plasma to very low levels. However, long-term therapy is associated with serious side effects, and interruption of therapy is generally associated with a rapid rebound of virus (6, 12, 13, 28, 38, 39), reflecting the long-term persistence of replication-competent virus (4, 8, 9, 47), persistent HIV-1 transcription in peripheral blood mononuclear cells (11), ongoing viral replication (15, 48), and the absence or failure of any persisting immune responses to control viral replication.

Both data and theory suggest that interrupting therapy in a structured manner to allow viral rebound can result in increased control of viral replication. A study of interrupting therapy in patients with acute HIV-1 infection showed that viral replication was controlled, either to undetectable or low, stable levels, accompanied by a restoration of CD4⁺-T-cell responses (37). A similar control of viremia to low levels has been observed in macaques experimentally infected with simian immunodeficiency virus after transient antiviral treatment (20) and structured treatment interruptions (STIs) (22) shortly after inoculation. Mathematical modeling of the dynamic interaction between the virus and the immune system (45, 46) has suggested that a change from a state of uncontrolled viral replication to one of sustained viral control is due to a switch

from CD4⁺ helper-independent CD8⁺ responses, which are insufficient to control viral replication, to a stronger, helper-dependent CD8⁺ response, which can suppress viral loads to low levels. Interrupting treatment during the early stages of infection can boost anti-HIV immune responses before damage to the CD4⁺ compartment due to viral replication has occurred. Although these models suggest that causing a switch to a powerful, helper-dependent CD8⁺ response will be much more difficult in the context of chronic infection, when the CD4⁺ compartment has already been damaged, anecdotal reports of patients with chronic HIV-1 infection who interrupted treatment in an unstructured manner suggest some improvement in HIV-specific CD8⁺-T-cell responses and even CD4⁺-T-cell responses (16, 27, 31, 32).

Nevertheless, there are also potential disadvantages to interrupting treatment. First, the burst of viral replication may result in a depletion of CD4⁺ T cells, which has been observed in interruptions of 3 months, although shorter (30-day interruptions) appear to have little effect (7, 39; L. Ruiz, J. Martinez-Picado, S. Marfil, K. Morales-Lopetegui, E. Ferrer, J. Romeu, and B. Clotet, 5th Int. Workshop HIV Drug Resist. Treatment Strategies, abstr. 40, 2001). Second, although theoretical studies suggest that new drug-resistant mutants are unlikely to evolve if there is limited replication during the interruption, this risk increases dramatically with the amount of viral replication (2). In addition, preexisting resistant virus may outgrow wild-type virus, as has been observed in two patients over three successive STIs (J. Martinez-Picado, K. Morales-Lopetegui, T. Wrin, S. Frost, C. J. Petropoulos, B. Clotet, and L. Ruiz, 5th Int. Workshop HIV Drug Resist.

* Corresponding author. Mailing address: Department of Pathology, Antiviral Research Center, 150 W. Washington St., Ste. 100, San Diego, CA 92103. Phone: (619) 543-5064, ext. 275. Fax: (619) 298-0177. E-mail: sdfrost@ucsd.edu.

Treatment Strategies, abstr. 36, 2001). Such a scenario can arise when the selective advantage of drug resistance during the on-therapy stage of the STI cycle outweighs the selective disadvantage of drug resistance mutations in the off-therapy stage. Third, viral reservoirs may also be reseeded during treatment interruptions. Although this may have limited pathogenic potential, since viral reservoirs are likely to persist throughout the lifetime of the infected individual, reseeding of reservoirs may archive genetic variation produced during interruption, facilitating viral evolution.

Given the central role that viral replication plays in the costs and benefits of treatment interruption (2), we need to have a good quantitative understanding of the viral population dynamics during interruptions. We present a detailed analysis of plasma viral load sampled frequently (median interval = 2 days) over four short (30-day) treatment interruptions, each followed by 90 days of highly active antiretroviral therapy (HAART), in a group of 12 chronically HIV-infected patients with a history of long-term viral suppression under HAART. We test the hypothesis that repeated STIs result in a decrease in viral replication rate by fitting a simple model of exponential growth to the viral load data from each individual. We employ a novel statistical approach, which allows us to obtain good estimates of (i) the viral growth rate, (ii) the time for virus to rebound to detectable levels, and (iii) residual error even when there are many viral load measurements below the limit of detection.

MATERIALS AND METHODS

Study population and design. The data analyzed here were obtained during a randomized, prospective STI study conducted at the Hospital Universitari Germans Trias i Pujol, Badalona, Spain. Full details of the selection criteria are given elsewhere (38, 39). In brief, 12 HIV-1-infected patients with a CD4/CD8 ratio of >1 sustained for a minimum of 6 months and who had HIV RNA levels in plasma of <50 copies/ml for at least 24 months before study entry were enrolled to interrupt their antiviral therapy in a structured manner. These criteria were chosen in order to enroll patients with well-conserved immunity and high levels of viral suppression. CD4⁺ counts ranged from 742 to 2,870 (median = 1,335) upon study entry. Treatment interruptions lasted for a maximum of 30 days, or until plasma viral loads were higher than 3,000 copies/ml in two consecutive determinations, after which HAART was resumed for ca. 90 days until the next STI cycle. In all cases, this resulted in suppression of plasma viremia to less than 50 copies/ml prior to the next interruption. HAART comprised of two nucleoside reverse transcriptase inhibitors (mainly lamivudine [3TC] and stavudine [d4T] [$n = 11$], but also zidovudine [ZDV] + didanosine [ddI] + hydroxyurea [$n = 1$]) and one protease inhibitor (mainly indinavir [IDV] [$n = 8$], but also nelfinavir [NFV] [$n = 2$], ritonavir [RTV] [$n = 1$], and saquinavir [SQV] [$n = 1$]). Thus, treatment regimes were fairly homogenous between patients. Patients who had received nonnucleoside reverse transcriptase inhibitors were excluded from the study, since the long half-life of this family of drugs may result in prolonged suboptimal concentrations during the early stages of treatment interruption, which may select for drug resistance mutations. Plasma HIV-1 RNA load was measured on frozen EDTA-plasma samples by using an Amplicor HIV-1 Monitor 1.5 (Roche Diagnostic Systems, Barcelona, Spain), with a limit of detection of 50 copies/ml. Viral load measurements were obtained frequently during the interruption period (median interval = 2 days, interquartile range = 2 to 3 days). Preliminary analysis revealed that in three patient-STI combinations (patient 4 [first STI cycle], patient 3 [fourth STI cycle], and patient 5 [third STI cycle]), the last viral load measurement taken was much lower than that expected under exponential growth. These measurements were removed from the statistical analysis, although this made little difference to our results.

Fitting an exponential growth model to pooled viral load data from each STI cycle. One approach to estimate viral dynamics parameters is to fit a model to viral load data pooled across individuals. In order to obtain meaningful average growth rates, we estimated the time between treatment interruption and viral loads becoming detectable (denoted "time to viral rebound" hereafter) for each

patient from the viral load data by taking the average of the times of the last undetectable viral load measurement and the first detectable viral load measurement. We then fitted a model of exponential growth to the viral load data obtained at each STI cycle, pooling data across individuals. If \bar{r}_j is the average viral growth rate at STI cycle j and t^* is the time since viral rebound, then the average log viral load, $\log[\bar{V}_j(t^*)]$ at time t^* is given by the equation $\log[\bar{V}_j(t^*)] = \log[\bar{V}_j(0)] + \bar{r}_j t^*$. Estimates of the average viral growth rate were obtained by using generalized least squares, correcting for nonindependence between measurements taken from each individual by using a continuous first-order autoregressive process and log-normal errors. We also tested for differences in the delay between different STI cycles by estimating the average delay in each STI cycle by using generalized least squares, correcting for repeated measurements on each individual by assuming a compound symmetry correlation structure. Patient-STI combinations where there was no viral rebound were excluded. Analyses were performed in R (<http://www.r-project.org>) by using the NLME library (35). Point estimates were obtained by using restricted maximum likelihood, and errors are given by approximate 95% confidence intervals (95% CI).

Fitting an exponential growth model to individual viral load data. Another approach of estimating viral dynamics parameters is to fit a model to each individual separately and then obtain average parameters. If we assume that the viral load grows exponentially in each patient at rate r_{ij} during treatment interruption, the log viral load in patient i at STI cycle j at time t (in days) after treatment interruption, $\log[V_{ij}(t)]$, is given by $\log[V_{ij}(t)] = \log[V_{ij}(0)] + r_{ij}t$.

We estimated the viral dynamics parameters from individual plasma viral load data by using a Bayesian approach, which is based on likelihood, and involves making prior assumptions about the parameter values in the model before performing the analysis. The main advantage of a likelihood-based method is that it allows us to include measurements below the limit of detection rather than omitting them or substituting them with arbitrary values such as the limit of detection (18, 23, 24). A Bayesian approach, where additional assumptions about the parameter values are made prior to the analysis, has some additional advantages over maximum-likelihood-based methods. First, it gives us the option to constrain parameter values in a highly flexible way. This can help to prevent overfitting of models by constraining parameters to biologically plausible values. This is particularly important when fitting models to individual viral load profiles, since relatively few measurements may be available for parameter estimation. Second, the output of a Bayesian analysis is a probability distribution known as the "posterior" (since it follows the analysis). Such probability distributions contain much more information about the parameter values than point estimates obtained by maximum likelihood and can be easily interpreted. A major criticism of a Bayesian approach is that the results (the "posterior distribution") may be more affected by the assumptions about the parameters (the "prior distribution") than they are by the data, which can occur if data are relatively sparse. In the following analysis, priors were chosen which were either "vague," in that they contain little information about the parameter, or they spanned a wide range of biologically plausible parameter values. Our results were found not to be sensitive to the priors. In part this was due to the highly frequent sampling of viral loads. Further discussion of the uses of a Bayesian approach in viral dynamics and evolution are provided elsewhere (3, 10).

We assumed that residual error in the log viral load was normally distributed with variance σ_{ij}^2 . Measurements below the limit of detection (50 copies of RNA/ml) were censored at the limit of detection. We considered a "fixed-effects" model, where no assumption is made about the distribution of between-patient variation in viral dynamics parameters. We fitted a "hierarchically centered" version of the model, $\log[V_{ij}(t)] = \log[V_{ij}(\hat{t})] + r_{ij}(t - \hat{t})$, where \hat{t} is the average of the measurement times, which reduces the amount of computer time required to fit to the model to a given accuracy. Vague normal distributions with means of 0 and variances of 10^6 were used for the prior distributions of $\log[V_{ij}(\hat{t})]$ and r_{ij} , the mean growth rate at each STI cycle. A uniform distribution in the range (0.01, 1) was used for the prior of the residual variance σ_{ij}^2 , corresponding to a standard deviation (SD) of between 0.1 and 1 \log_{10} copies/ml. This range encompasses measurement error (0.18 \log_{10} copies/ml) (40), the minimum residual error expected, and the level of variation in viral load measurements observed at the viral setpoint in untreated individuals (ca. 0.6 \log_{10} copies/ml) (25).

To validate our method, we compared our parameter estimates with those obtained by using normal least-squares methods which omitted measurements below the limit of detection. We calculated the time taken for viral loads to increase to detectable levels (50 copies/ml; denoted by "time to viral rebound") by using our model estimates and least-squares estimates of the slope and intercept with the following expression: $\log(50) - \log[V_{ij}(0)]/r_{ij}$. Predicted times of viral rebound of <0 (i.e., before treatment interruption) were set to zero. The difference between the time of viral rebound estimated directly from the data (by using the times of the last undetectable and the first detectable viral load mea-

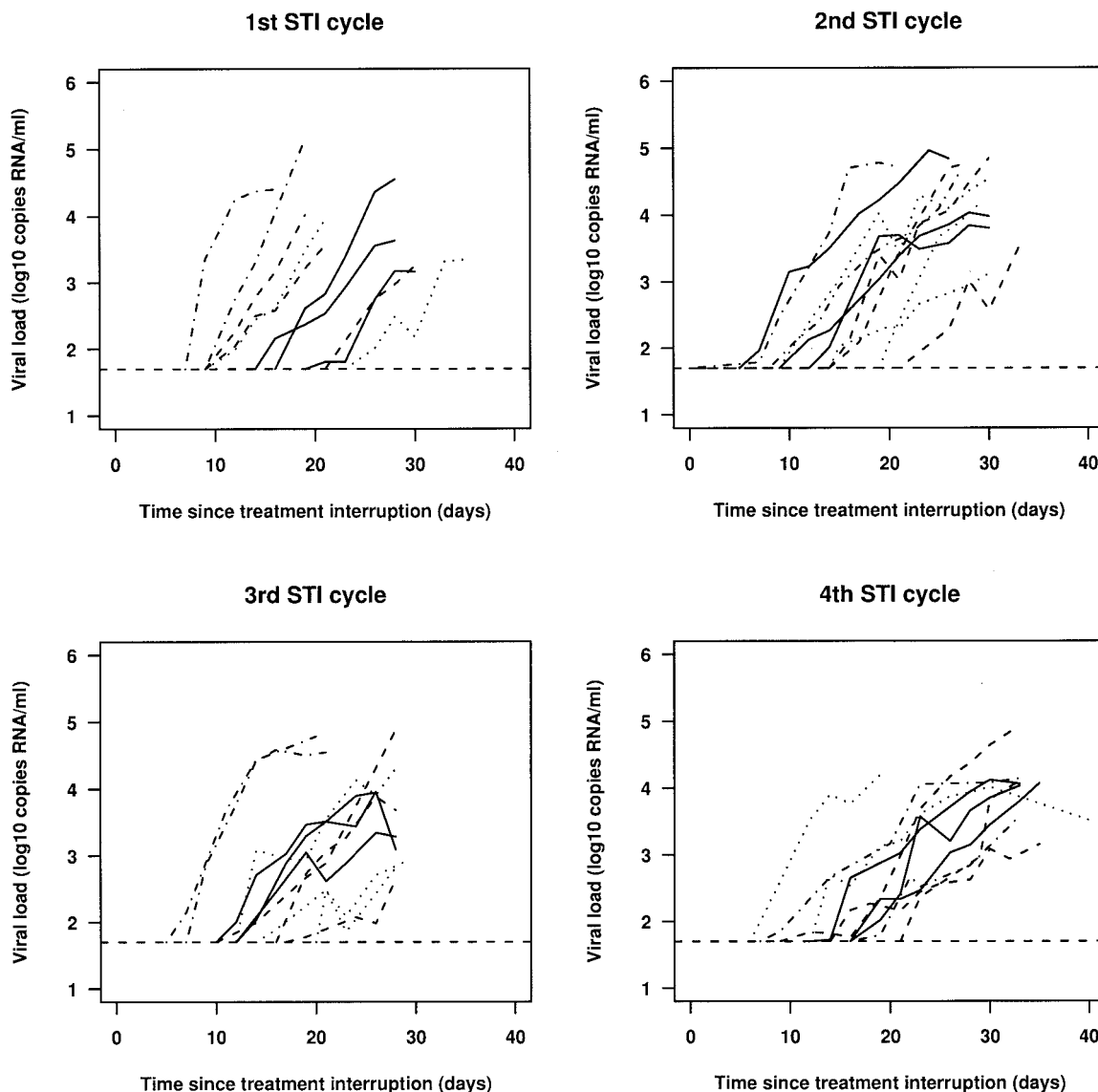


FIG. 1. Viral loads in plasma (expressed as \log_{10} copies/ml of plasma) over time (in days) over four cycles of treatment interruption in 12 chronically HIV-1-infected patients. The dotted horizontal line represents the limit of detection of the viral load assay (50 copies/ml). Interruption cycles without any detectable virus are excluded.

surements) and that predicted by the model estimates (both with our Bayesian method of parameter estimation and least squares) was used to indicate the goodness-of-fit of the model.

Our model cannot be fitted by using analytical formulae, and so instead we obtained a sample of parameter values from the posterior distribution by using a Monte Carlo Markov Chain method. Full details of such an approach can be found elsewhere (14). In brief, rather than producing a set of random, independent samples from the posterior distribution, a Markov Chain produces a chain of correlated samples, starting off from a set of initial values. Model fitting was performed by using WinBUGS v.1.3 (42). The length of the Markov Chains to be run was chosen to give estimates of the 2.5 and 97.5 percentiles of the marginal posterior distribution of each parameter to within 1% (except for the residual standard deviation, for which the Markov Chain mixed poorly, i.e., produced a highly autocorrelated sample, resulting in a low effective sample size). In order to verify that the results were not affected by the choice of initial conditions used to start the Markov Chain, convergence analysis was performed by using the Coda package (36) in R (<http://www.r-project.org>). We summarized the output of the model (the full joint distribution of the parameters) by calculating the "marginal distributions" for each parameter, which integrate out the uncertainty

in the other parameter estimates. Point estimates of parameters were obtained by calculating the median of the marginal distributions, and a 95% error bound on each parameter was obtained by using the 2.5 and 97.5 percentiles. For graphical purposes, smoothing of the marginal posterior distributions was performed by using the KernSmooth (43) package in R.

RESULTS

Summary of data. Plasma viral load measurements were obtained very frequently (median interval 2 days) from each patient during each of the four treatment interruptions. Of the 12 patients who underwent treatment interruptions, one showed no rebound in any of the four interruptions (patient 9), one did not show a rebound in the first STI cycle (patient 12), and one did not show a rebound in the fourth interruption (patient 6). The dynamics of viral rebound over the four interruptions is shown in Fig. 1.

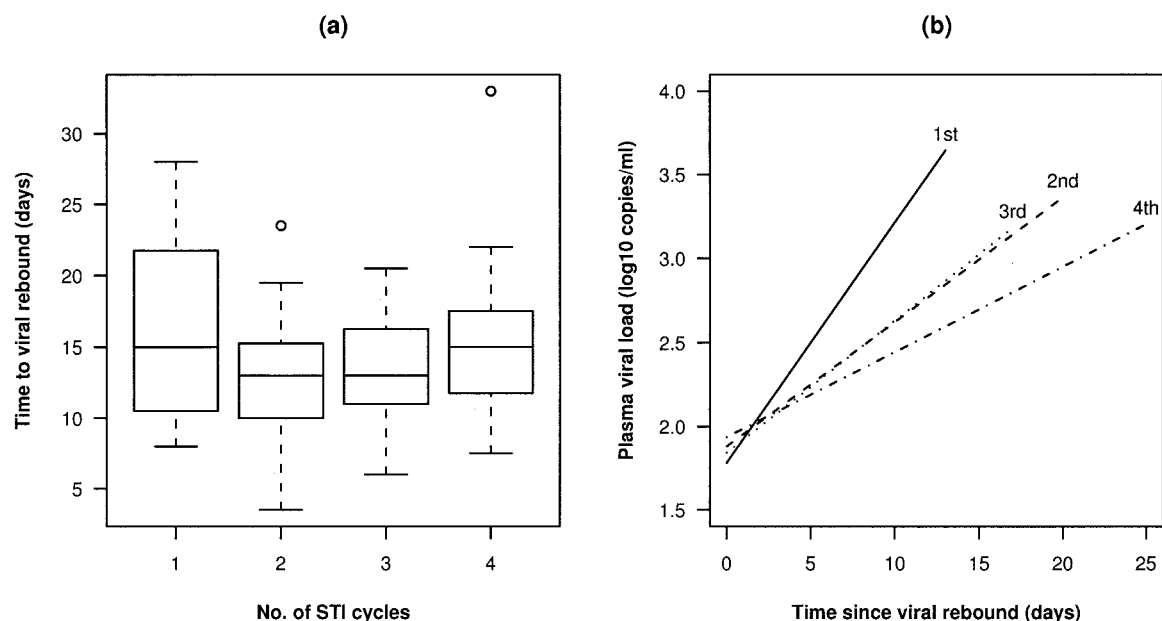


FIG. 2. (a) Box-and-whisker plot of the time to viral rebound, for each patient across four cycles of treatment interruption, calculated by using the average of the times of the last undetectable and the first detectable viral loads. The boxes span the second and third quartiles, and the whiskers extend to the most extreme data point that is no more than 1.5 times the interquartile range from the box. Patient 9, who showed no rebound during any of the four interruptions, is omitted. The time to viral rebound for patient 12 in the first STI cycle and patient 6 in the fourth STI cycle (when virus did not rebound during the interruption) is given conservatively by the length of the interruption. (b) Fitted values for the average viral load over time since viral rebound across four STI cycles. Estimates of the average growth rates were as follows: first cycle, 0.22 log₁₀ copies/ml/day (0.18 to 0.26, 95% CI); second cycle, 0.16 log₁₀ copies/ml/day (0.13 to 0.18, 95% CI); third cycle, 0.16 log₁₀ copies/ml/day (0.13 to 0.19, 95% CI); and fourth cycle, 0.12 log₁₀ copies/ml/day (0.09 to 0.14, 95% CI).

Estimates of the average viral growth rate during each STI cycle. Since the time between treatment interruption and detection of viral loads, which we denote “time to viral rebound,” is highly variable between individuals, it is difficult to visually compare the rates of viral outgrowth across STI cycles directly from Fig. 1. Hence, we estimated the time to viral rebound for each patient by using the average of the times of the last undetectable and first detectable viral load measurements and then fitted a model of exponential viral growth based on the time since viral rebound rather than the time since treatment interruption (Fig. 2). We pooled viral load measurements from different individuals to obtain an average growth rate for each STI. The viral growth rate was high in the first STI cycle (0.219 log₁₀ copies/ml/day), intermediate in the second and third STI cycles (0.156 and 0.158 log₁₀ copies/ml/day, respectively), and lowest in the fourth STI cycle (0.115 log₁₀ copies/ml/day). On average, the viral load in the fourth STI cycle is nearly half that in the first STI cycle ($P < 0.01$ against the null hypothesis of no difference in growth rates). The average time to viral rebound in the first STI cycle was 15.6 days, with slightly shorter times in subsequent cycles (12.9, 13.3, and 14.8 days in the second, third, and fourth STI cycles, respectively), although the difference was only significant between the first and second STI cycles ($P < 0.05$) (Fig. 2).

Obtaining viral dynamics estimates for each individual. Average viral dynamics parameters can be easily obtained by a “top down” approach, where data from different individuals are pooled together, even when the number of data points per individual is small, provided a suitable correction for repeated measurements is made. However, by averaging across patients,

biologically interesting variation between individuals in viral dynamics may be obscured. The viral dynamics in the first and fourth STI cycles for each patient are shown in Fig. 3, which illustrates extensive variation, both within and between STI cycles. In such cases, a “bottom up” approach may be desirable, where parameters are estimated from each individual, with subsequent statistical analysis of the averages of individual parameter estimates (see, for example, references 13, 17, 33, 34, and 44).

Most previous studies have obtained individual level parameter estimates by using standard least-squares methods, which cannot easily deal with measurements below the limit of detection. Such measurements are either omitted or substituted with an arbitrary value, such as the limit of detection. However, such an approach does not work well when there are many viral load measurements below the limit of detection (18, 23, 24), since it results in biased parameter estimates and a loss of statistical power.

We have instead estimated individual viral dynamics parameters by using a Bayesian approach, which combines prior assumptions of parameter values with the likelihood of the data given the model to produce a joint probability distribution of the model parameters. Viral load measurements below the limit of detection are included in the model by averaging over all of the possible values below the limit of detection, and biologically reasonable constraints can be placed on the parameters in order to reduce bias and increase power. A simple exponential model of viral growth was found to give a good fit to the viral dynamics during the short interruption periods.

The output of our analysis is a joint probability distribution

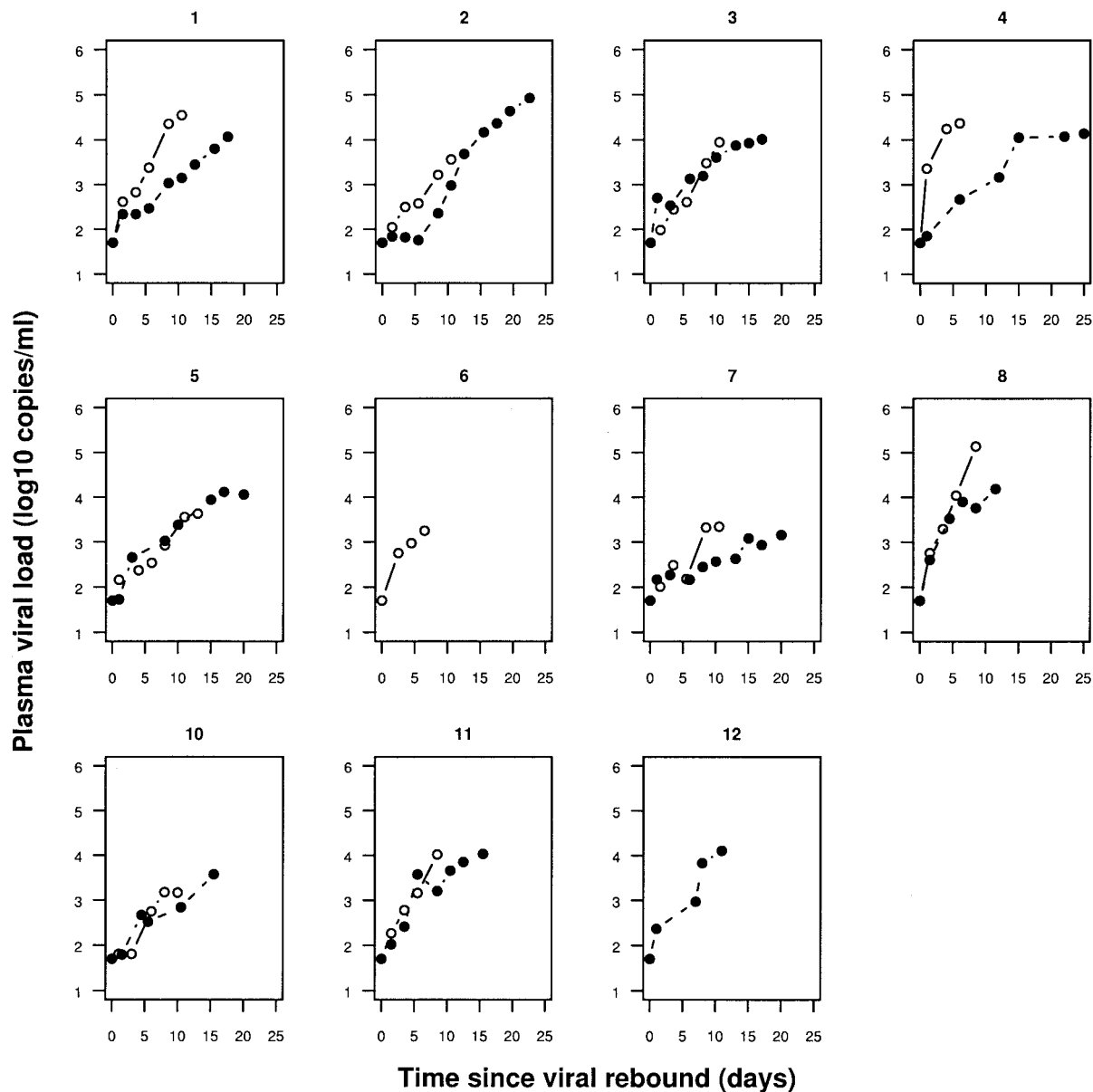


FIG. 3. Viral loads in plasma (in \log_{10} copies/ml) for each of the patients in the first interruption (\circ) and the fourth interruption (\bullet) over time since viral rebound. There was no rebound in the first interruption in patient 12, and no rebound in the fourth interruption in patient 6.

of viral dynamics parameters for each individual. These distributions were approximated by sampling from the distributions by using a computational method known as the Monte Carlo Markov Chain. For the data presented here, it was computationally intensive to produce a sample of viral dynamics parameters which gave a good approximation to the probability distributions of the parameters. To test the extent of improvement in estimates of viral dynamics parameters obtained by using our Bayesian approach compared to a much simpler and faster least-squares approach, we implemented a simple goodness-of-fit test. The times to viral rebound estimated directly from the data (Fig. 2) were compared with estimates by using an exponential growth model fitted by (i) our Bayesian approach (which included time points with undetectable viral loads) and (ii) by using least squares (which omitted all time

points with undetectable viral loads). Since viral loads were sampled very frequently, estimates of the time to viral rebound obtained directly from the data are likely to be reasonably accurate, and hence comparison of these estimates with those expected under a given model indicates how well the model fits. Point estimates of time to viral rebound obtained by using our Bayesian approach were very close to estimates obtained directly from the data (median difference = -0.44 days, range = -2.57 to $+3.44$ days). However, the time to viral rebound was underestimated, in some cases quite dramatically, by using a least-squares approach (median difference = -2.99 days, range = -18 to $+2.75$ days; Fig. 4), with corresponding underestimates of the viral growth rates (data not shown). In addition, since the number of undetectable viral loads varied between individuals and across STI cycles, variation between

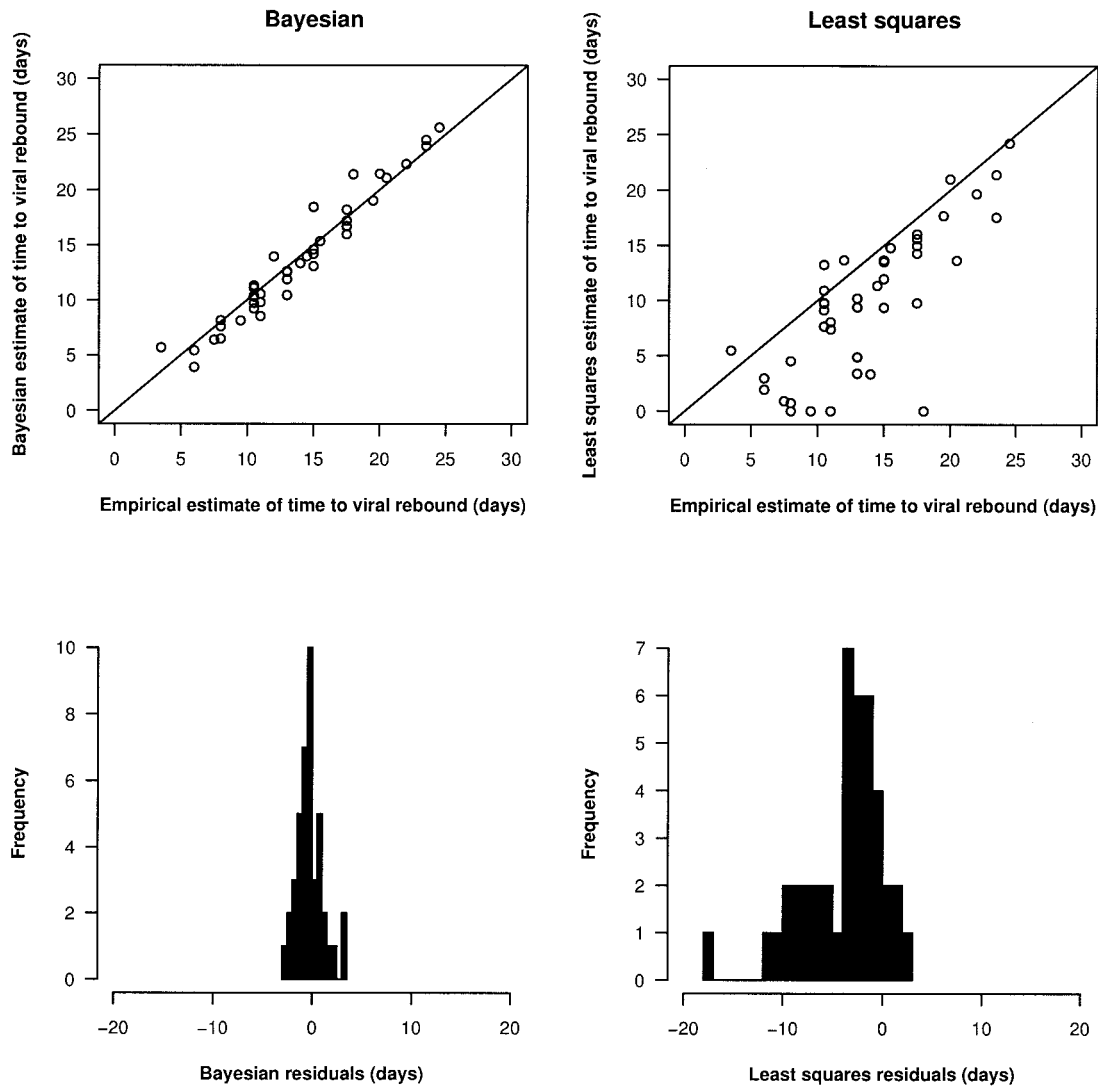


FIG. 4. Comparison of empirical estimates of the time to viral rebound with model estimates (at the top) and residual plots (at the bottom) obtained by fitting a model of exponential viral growth by using our Bayesian approach (on the left) and by using a least-squares approach (on the right). Bayesian estimates correlated well with the empirical estimates, whereas least squares gave underestimates of the time to viral rebound. Bayesian point estimates were calculated by using the median of the marginal posterior probability distribution. Negative delays (which were obtained for some interruption cycles for some patients by using least squares) were replaced by zero.

individuals in estimates of viral growth rate could be generated by different levels of parameter bias rather than real biological effects, stressing the importance of inclusion of undetectable viral loads.

Viral dynamics after viral rebound over successive treatment interruptions. Having validated our approach of parameter estimation, we estimated the viral growth rate for each individual at each STI cycle. Over the course of the four STI cycles, the viral growth rate decreased from an average of 0.29 \log_{10} copies/ml/day (0.24 to 0.35, 95% interval) in the first interruption to 0.15 \log_{10} copies/ml/day (0.13 to 0.18, 95% interval), excluding patient 12 in the first STI cycle, and patient 6 in the fourth STI cycle, who did not demonstrate a viral rebound (Table 1). These averages take into account errors in the estimates of growth rates at an individual level, in contrast to many studies that analyze individual estimates obtained by

least squares as if they were not subject to estimation error. While these estimates are slightly higher than those obtained by pooling individual data, they are in broad agreement, demonstrating an approximate halving of the viral growth rate over four STI cycles. Plotting the full probability density distributions provides a simple graphical way of illustrating variation between individuals in parameter estimates (Fig. 5). This illustrates that, for example, there are two patients in the first STI cycle that appear to exhibit a very high viral growth rate (corresponding to patients 4 and 8 in Fig. 3), although the errors with these estimates are high (as shown by the broadness of the distributions).

We calculated the basic reproductive rate, R_0 , defined as the number of secondary productively infected cells produced by a single productively infected cell, which gives an indication of the effect of treatment interruption on the reduction in viral

TABLE 1. Summary of estimates of viral dynamics parameters over four STI cycles^a

Parameter	Results with (no. of STI cycles):			
	1	2	3	4
Avg growth rate (\log_{10} copies/ml/day) (95% interval) ^b	0.288 (0.240, 0.349)	0.189 (0.167, 0.218)	0.191 (0.163, 0.226)	0.154 (0.134, 0.181)
R_0 (no delay) ^c (% relative to first STI)	2.33 (100)	1.87 (80.4)	1.88 (80.8)	1.71 (73.5)
R_0 (fixed delay) ^d (% relative to first STI)	3.23 (100)	2.22 (68.7)	2.24 (69.2%)	1.93 (59.8%)
Avg time to viral rebound (days) ^e (95% interval)	15.2 (14.3, 16.0)	12.2 (11.0, 13.3)	13.6 (12.4, 14.8)	13.6 (12.3, 14.8)
Predicted initial viral load (\log_{10} copies/ml) ^f (95% interval)	-2.38 (-3.78, -1.51)	-0.81 (-1.58, -0.81)	-0.84 (-1.61, -0.25)	-0.48 (-1.11, -0.02)
No. of patients with residual SD greater than the measurement error/total no. ^g	2/10	7/11	9/11	7/10

^a We excluded patient 12 in the first interruption and patient 6 in the fourth interruption, since there was no viral rebound detected at these interruptions.

^b The 95% interval is given as follows: lower value, upper value.

^c The viral basic reproductive rate, R_0 , defined as the number of secondary productively infected cells produced by a single infected cell when the number of infected cells is small, was estimated by using the “standard model of viral dynamics” (29), assuming no delay between the infection of a target cell and the production of virions and an average viral production time of 2 days.

^d The viral R_0 was calculated by using a model which has a fixed delay (of 1 day) between infection of a target cell and production of virions (30), followed by a period of viral production (with an average duration of 1 day).

^e The time to viral rebound is defined as the time between treatment interruption and viral load reaching 50 copies/ml.

^f The predicted initial viral load was estimated by extrapolating exponential growth back to the beginning of the interruption period.

^g The residual SD is defined as higher than measurement error when the 95% interval does not overlap 0.18 \log_{10} copies/ml (38), resulting in a conservative (two-sided) test.

replication. Under the “standard” model of viral dynamics (29), R_0 can be calculated from the rate of viral rebound, r (in \log_e units), by using the expression $R_0 = 1 + rD$, where D is the average lifetime of an infected cell. The standard model makes a number of simplifying assumptions, which when relaxed can lead to very different estimates of R_0 for a given value of r (21). If we assume a fixed delay between infection of a cell and production of virus, of length D_1 , followed by an exponentially distributed period of viral production of average length D_2 , R_0 is given by the expression $R_0 = (1 + rD_2)\exp(rD_1)$ (30). If we assume $D = D_1 + D_2 = 2$ days, the estimated decrease in the average growth rate from 0.29 to 0.15 \log_{10} copies/ml/day over the course of four STI cycles is equivalent to a decrease in viral R_0 from 2.3 to 1.7 under the standard model of viral dynamics and from 3.2 to 1.9 under a fixed-delay model (Table 1). Given that $CD4^+$ counts at the beginning of each interruption were similar for all four interruptions (39), this decrease in viral R_0 is likely to be due to increases in HIV-specific immune responses rather than to decreases in target cell availability.

We also estimated the residual SD, which represents the scatter of viral load measurements about our model (Fig. 6). Estimates of residual SD which are close to those expected under measurement error alone indicate smooth exponential growth. High estimates of residual SD represent very “noisy” viral load trajectories, which could be caused by fluctuations in target cells and/or HIV-specific immune responses. Our approach allowed us to constrain estimates of residual SD to lie between 0.1 and 1 \log_{10} copies/ml, allowing us to obtain estimates for each patient individually with a relatively small number of data points. These bounds were chosen to reflect the range of biologically reasonable values of variation in viral loads, encompassing measurement error of the Roche AmpliCor assay used in the study (0.18 \log_{10} copies/ml) (40) and the amount of variation typically observed in untreated HIV-1-infected patients at the viral setpoint (0.6 \log_{10} copies/ml) (25).

On average, the residual SD increased over the course of the four STI cycles (Fig. 5). This can be seen in the plots of the viral load trajectories in Fig. 1 and 3 as a larger number of

spontaneous drops in viral load in later cycles. During the first interruption, the residual SD in the first STI cycle was not significantly different from measurement error in 8 of 10 patients. In contrast, by the fourth STI cycle, the residual SD was significantly higher than measurement error in 7 of 10 patients (Table 1). The increase in residual SD above that expected under measurement error alone is due to changes in the rates of viral production and/or clearance over the course of the fourth interruption. We hypothesize that these short-term fluctuations in viral load could arise due to fluctuations in HIV-specific immune responses.

DISCUSSION

We have analyzed in detail the dynamics of viral rebound in 12 chronically HIV-1-infected individuals who underwent four rounds of STI. Our data set is unusual compared to many studies of treatment interruption in that viral load measurements were obtained very frequently. To characterize the extensive variation in viral growth between individuals, we took a common approach of fitting a model of exponential growth to viral load data from each individual (13, 17, 33, 34, 44). However, in contrast to many studies of viral dynamics, we fitted a Bayesian version of this model, which allows us to include measurements below the limit of detection and to place constraints on parameter values, which reduced the problem of overfitting the model.

The dynamics of viral outgrowth after detection in the plasma were well characterized by a simple model of exponential growth. The average viral growth rate approximately halved between the first and fourth interruptions, representing a significant drop in viral basic reproductive rate, especially when realistic models of the viral life cycle are considered. This effect is underestimated if viral load measurements are omitted from the analysis and may be biased if such measurements are replaced with ad hoc values; hence, we adopted a model-fitting approach that can include viral load measurements below the limit of detection while allowing for uncertainty in the true

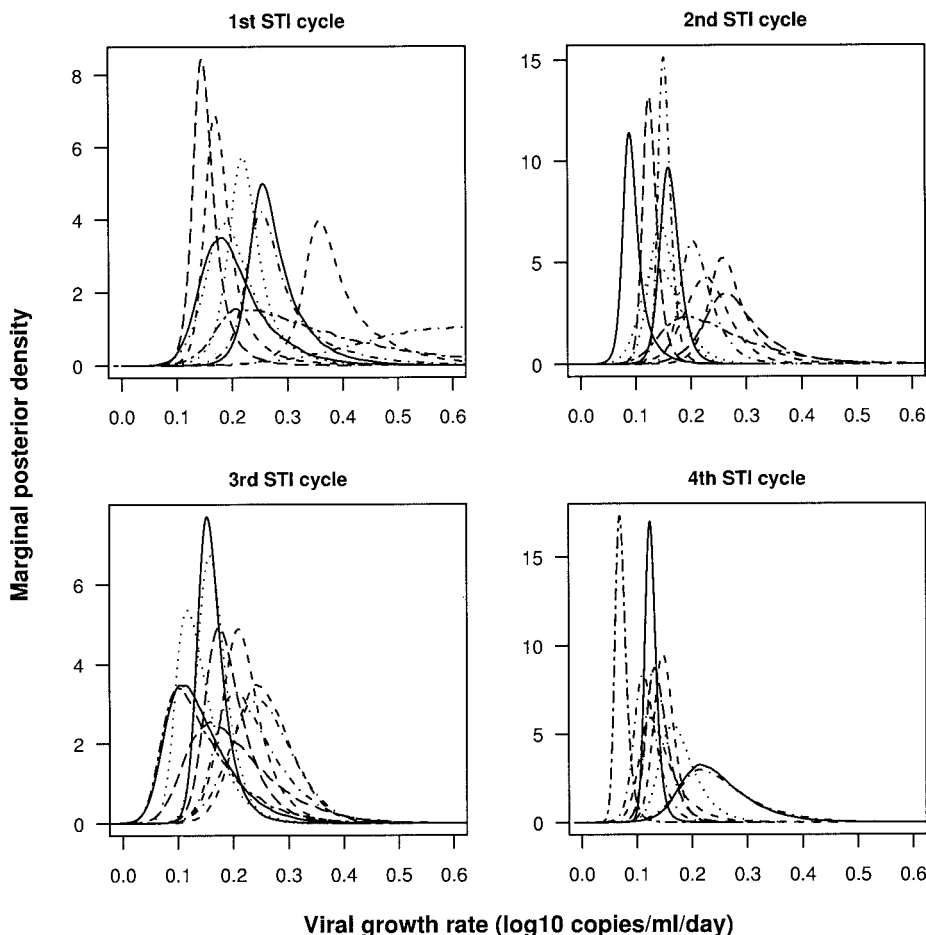


FIG. 5. Marginal posterior probability density plot of the estimates of viral growth rate in plasma (in log₁₀ copies/ml/day) for each patient across four cycles of treatment interruption. The rate of viral outgrowth on average decreased over successive STI cycles.

value. The reduction in viral replication is unlikely to be due to lower target cell concentrations. Although the level of circulating CD4⁺ cells decreased slightly over the course of a given STI cycle, there was not a progressive decrease in CD4⁺ cells over the course of the STI cycles (39). Given that the viral load generally failed to reach the individual pretherapy setpoint during each interruption (data not shown), the number of target cells is not likely to be a limiting factor. One possible explanation for the drop in R_0 is that HIV-specific immune responses increased over multiple STI cycles. Given that viral growth was suppressed even when viral loads were very low, it seems likely that the lower rate of viral outgrowth is due to HIV-specific immune responses present at the beginning of the interruption, which accumulate over the course of multiple STI cycles. This is consistent with an observed increase in the number of activated CD8⁺ CD38⁺ T cells present at the beginning of each interruption increased over multiple cycles, although HIV-specific CD8⁺-T-cell responses measured by ELISPOT against a panel of epitopes increased in only a minority of these patients (39).

In addition, there was an increase in viral fluctuations around exponential growth in later STI cycles, as shown by an increase in the residual SD above that expected under measurement error. The detection of this effect was aided by the

ability of our model to include biologically reasonable constraints on the possible range of the residual SD. Such fluctuations in viral load are due to fluctuations in the rate of viral production and/or clearance. In the context of viral outgrowth, the trend toward greater fluctuations in later STI cycles suggests that these may be due to short-term fluctuations in HIV-specific immune responses, implying a highly dynamical interaction between HIV and the immune response.

The dynamics of viral replication in the very early stages of interruption are also of interest and are particularly relevant to STI protocols comprising multiple, short interruptions intended to reduce exposure to drug, while minimizing the risk of viral rebound (M. Dybul, T. W. Chun, C. Yoder, M. Belson, B. Hidalgo, K. Hertogs, B. Larder, C. Fox, J. Orenstein, J. Metcalf, R. Davey, C. Hallahan, R. Dewar, M. Baseler, and A. S. Fauci, 8th Conf. Retrovir. Opportunistic Infect., abstr. 354, 2001). By obtaining frequent viral load samples, we were able to estimate the time between treatment interruption and viral loads reaching the limit of detection with a narrow margin of error. We demonstrated that despite an approximate halving of the average growth rate of virus over four STI cycles, the average time to viral rebound was not significantly different between the first and fourth STI cycles and even shows a significant decrease between the first and second STI cycles.

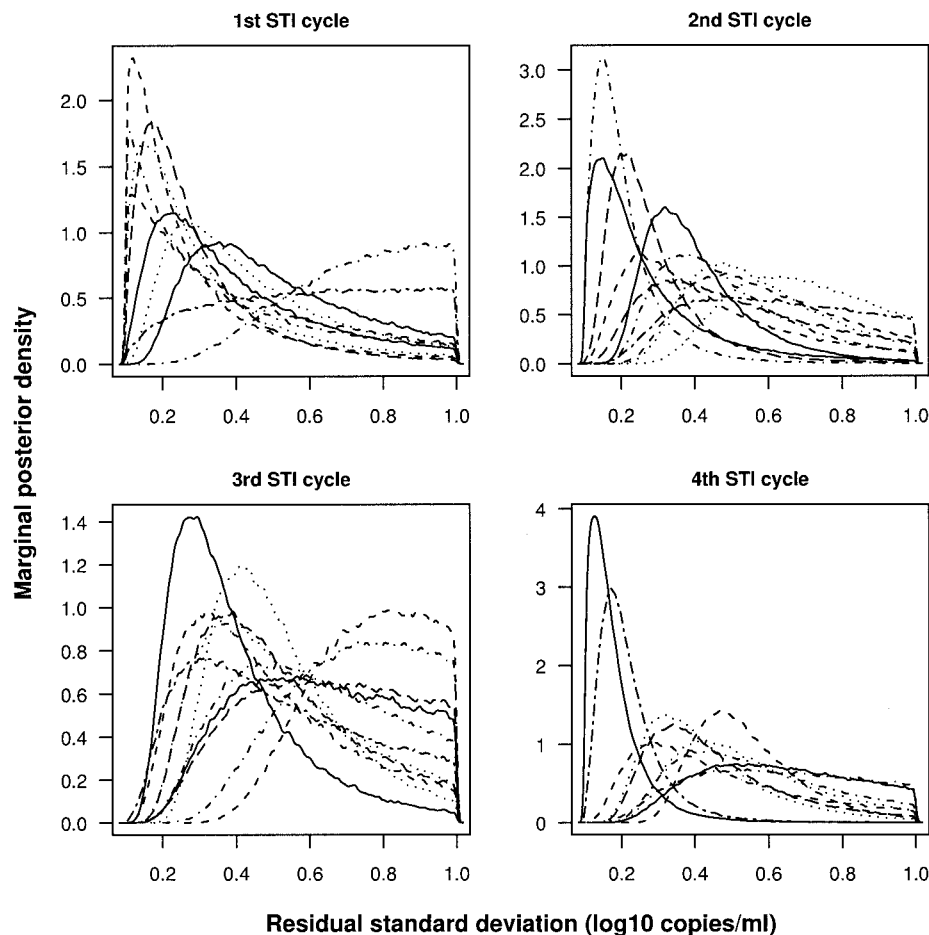


FIG. 6. Marginal posterior probability density plot of the residual SD, representing the scatter of viral load measurements around smooth exponential growth (in \log_{10} copies/ml) for each patient across four cycles of treatment interruption. The residual SD on average increased over successive STI cycles.

One possible explanation for this discrepancy is that the growth rates above and below the limit of detection were the same, but the viral load present at the beginning of the interruption increased over successive STI cycles. By extrapolating back, we can use our model to predict the viral load present at the beginning of the interruption based on the assumption of exponential growth throughout each interruption. Figure 7 shows the probability distribution of the predicted viral load at the time of treatment interruption (“initial viral load”). On average, the initial viral load predicted by this model increased by nearly 2 logs between the first and fourth STI cycles (Table 1).

An increase in the viral load present prior to interruption could be due to the reseeding of viral reservoirs. Given that the patients had previously suppressed viremia to below detectable levels for 2 years, viral reservoirs with half-lives on the order of months would have been very low prior to the study, while longer-lived reservoirs are likely to be saturated. Since the duration of treatment between interruptions was approximately 3 months, viral reservoirs with lifetimes of days to weeks are likely to have decayed to low levels prior to the next interruption. Based on this reasoning, we hypothesize that the increase in predicted initial viral load could arise due to an

increase in viral reservoirs with intermediate half-lives of the order of several months. Any new drug resistance mutations that emerge during treatment interruptions may be archived in these reservoirs, which could lead to the rapid emergence of a resistant viral population in response to subsequent treatment. In order to test this hypothesis, the reservoirs that initiate viral rebound need to be quantified. This is hampered by our lack of knowledge on the identity of these reservoirs. Genetic differences between rebounding plasma virus and latently infected cells in the blood have been demonstrated in some but not all patients (5, 19, 49), suggesting that the rebounding virus may not originate from the blood, at least in these patients. Virus bound to follicular dendritic cells, which can remain infectious for long periods of time even during suppressive therapy (41), may be a potential source of the rebounding virus.

Model estimates of the viral load present at the beginning of the interruption obtained by extrapolation are based on the assumption of deterministic exponential growth throughout the interruption. “Back-of-the-envelope” calculations suggest that this may be an unrealistic assumption, at least for a subset of patient-STI combinations. Some estimates of initial viral load appear very low, especially in the first STI, where point estimates of the initial viral loads were less than -2 logs in 5

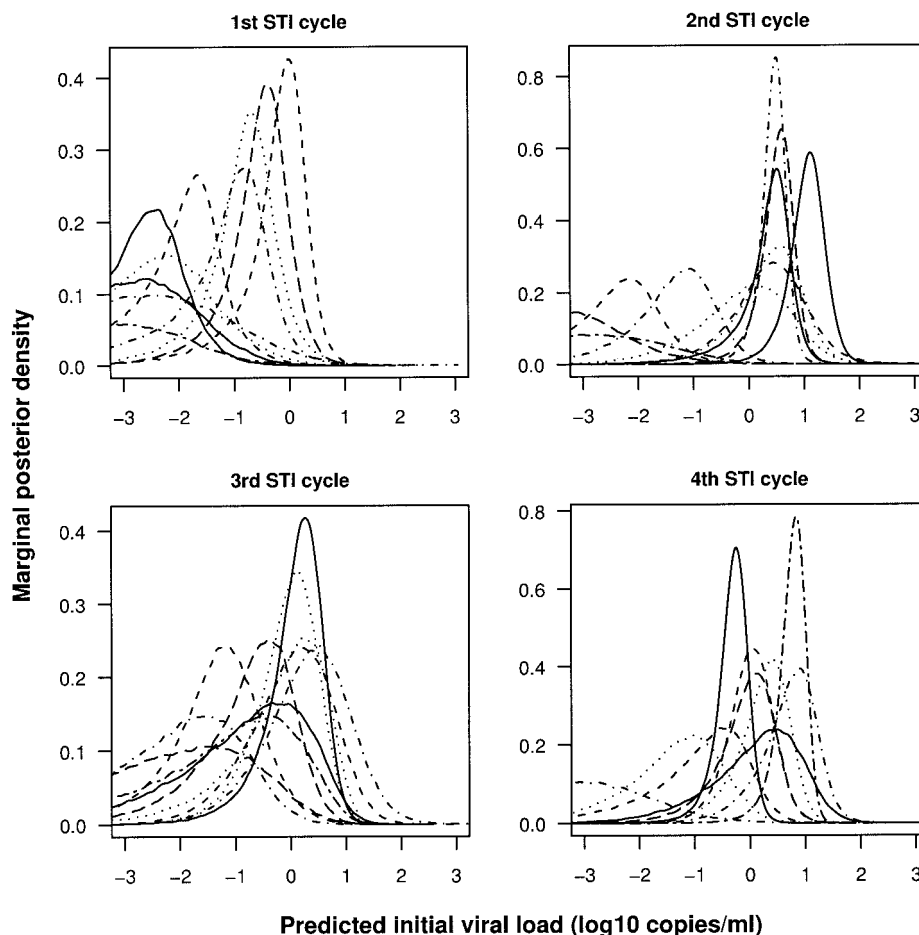


FIG. 7. Marginal posterior probability density plot of the initial viral load as predicted assuming exponential growth throughout each interruption cycle (in \log_{10} copies/ml) for each patient across four cycles of treatment interruption. The predicted initial viral load increased over successive STI cycles.

individuals out of 10. If we assume 5 liters of blood, 65% of which is plasma, a viral load of $-2 \log_{10}$ copies/ml is equivalent to only 16 free virions. It is possible that the levels of virus in solid tissue that correspond to this level in the blood are low enough that the virus does not grow deterministically throughout the whole interruption but rather fluctuates stochastically, at least in the initial stages of interruption. This could result in long delays between treatment interruption and viral loads reaching detectable levels simply due to chance, which in turn would result in underestimates of initial viral load. However, as stochastic effects average out across individuals, our conclusion that there is a trend toward higher initial viral loads remains robust under the assumption of initial stochastic rather than deterministic growth.

In addition, one individual (patient 6) failed to show a rebound in the fourth interruption after 33 days of interruption, despite showing viral rebounds in the previous interruptions (after 23.5, 23.5, and 18 days after interruption in the first, second, and third interruptions, respectively). The long delay in this patient in the fourth STI cycle may represent immune control of replication over the period of interruption rather than stochastic outgrowth from a small population. We hypothesize that HIV-specific immune responses present at the

beginning of the interruption dominate during the early stages of interruption, with additional responses being induced only when the viral load is close to setpoint. With this hypothesis, HIV-specific immune responses may be relatively constant during the early stages of interruption, such that lower growth rates after rebound would be associated with longer times to viral rebound. Hence, even though immune responses may determine the rate of viral outgrowth, reseeding of viral reservoirs needs to be invoked to explain the relative constancy across STI cycles of time to viral rebound. Frequent sampling of HIV-specific immune responses is needed to determine the level of immune responses prior to interruption, the dynamics of induction of additional responses, and whether short-term fluctuations in viral load during outgrowth are correlated with fluctuations in HIV-specific immunity.

Our results suggest that the effect of STIs in chronically infected patients on viral replication is modest compared to the effect of STIs during primary infection or compared to the effects of successful treatment. Despite trends in viral dynamics parameters averaged across patients over successive STI cycles, we have shown extensive between-patient variation in these parameters, a finding consistent with other studies of STIs in chronically infected patients (13; C. Fagard, M. Lebraz,

H. Günthard, C. Tortajada, F. Garcia, M. Battegay, H. J. Furrer, P. Vernazza, E. Bernasconi, L. Ruiz, A. Telenti, A. Oxenius, R. Phillips, S. Yerly, J. Gatell, R. Weber, T. Perneger, P. Erb, L. Perrin, and B. Hirschel, 8th Conf. Retrovir. Opportunistic Infect., abstr. 357, 2001), and further investigation is needed to identify the causes of this variation. It is possible that the variable response to treatment interruptions reflects the nature of the rebounding virus. If the rebounding virus is antigenically similar across interruptions, we hypothesize that this may boost HIV-specific immune responses more than if different viral antigenic variants rebounded in different interruptions. In addition to the lack of restoration of CD4⁺-T-cell responses, the rebound of distinct viral variants over subsequent interruptions could also contribute to the overall modest effect of STIs in chronically infected patients, in whom the virus is genetically diverse, relative to patients with acute infection, in whom viral diversity may be low due to the initial bottleneck of infection. Treatment interruptions have also been proposed as a regimen that may minimize exposure to antiviral agents and hence reduce side effects (Dybul et al., 8th Conf. Retrovir. Opportunistic Infect., abstr. 354) and also as a regimen that would allow the reversion of drug-resistant virus to wild type in individuals harboring highly resistant virus, which may increase the response to a salvage regimen (1, 7, 26). Determination of the interruption protocol involves the weighing of costs and benefits of treatment interruptions, which involves consideration of the dynamics of replication of virus during interruption as follows: (i) multiple, short interruptions may be desirable to reduce exposure to drug, while minimizing the risk of viral rebound; (ii) a single, long interruption may be required to allow sufficient replication for the reversion of resistant virus to wild type; and (iii) multiple interruptions of intermediate length may be required to allow sufficient rebound of virus to stimulate immune responses, while minimizing the risk of damage to the CD4⁺ compartment. The application of more sophisticated methods of fitting viral dynamics models to data from these interruption studies will help us to understand more about the dynamics of viral rebound, how it varies between individuals, and whether STIs or similar strategies may be viable in a clinical context.

ACKNOWLEDGMENTS

This research was supported by grants AI47745 (S.D.W.F. and A.J.L.B.) and TW00767 (Fogarty Center) (A.J.L.B.) from the National Institutes of Health and by grants FIPSE 3025/99, FIPSE 36177/01, and FIS 01/1122. J.M.-P. was supported by contract FIS 99/3132 from the "Fundacio per a la Recerca Biomedica Germans Trias i Pujol" in collaboration with the Spanish Health Department.

REFERENCES

1. Altfeld, M., and B. D. Walker. 2001. Less is more? STI in acute and chronic HIV-1 infection. *Nat. Med.* 7:881–884.
2. Bonhoeffer, S., M. Rembiszewski, G. M. Ortiz, and D. F. Nixon. 2000. Risks and benefits of structured antiretroviral drug therapy interruptions in HIV-1 infection. *AIDS* 14:2313–2322.
3. Burroughs, N. J., D. Pillay, and D. Mutimer. 1999. Significance testing of clinical data using virus dynamics models with a Markov Chain Monte Carlo method: application to emergence of lamivudine resistant hepatitis B virus. *Proc. Natl. Acad. Sci. USA* 266:2359–2366.
4. Chun, T. W., L. Stuyver, S. B. Mizell, L. A. Ehler, J. A. M. Mican, M. Baseler, A. L. Lloyd, M. A. Nowak, and A. S. Fauci. 1997. Presence of an inducible HIV-1 latent reservoir during highly active antiretroviral therapy. *Proc. Natl. Acad. Sci. USA* 94:13193–13197.
5. Chun, T. W., R. T. Davey, M. Ostrowski, J. S. Justement, D. Engel, J. I. Mullins, and A. S. Fauci. 2000. Relationship between pre-existing viral reservoirs and the re-emergence of plasma viremia after discontinuation of highly active anti-retroviral therapy. *Nat. Med.* 6:757–761.
6. Davey, R. T., Jr., N. Bhat, C. Yoder, T. W. Chun, J. A. Metcalf, R. Dewar, V. Natarajan, R. A. Lempicki, J. W. Adelsberger, K. D. Millers, J. A. Kovacs, M. A. Polis, R. E. Walker, L. Falloon, H. Masur, D. Gee, M. Baseler, D. S. Dimitrov, A. S. Fauci, and H. C. Lane. 1999. HIV-1 and T-cell dynamics after interruption of highly active antiretroviral therapy (HAART) in patients with a history of sustained viral suppression. *Proc. Natl. Acad. Sci. USA* 96:15109–15114.
7. Deeks, S. G., T. Wrin, T. Liegler, R. Hoh, M. Hayden, J. D. Barbour, N. S. Hellman, C. J. Petropoulos, J. M. McCune, M. K. Hellerstein, and R. M. Grant. 2001. Virologic and immunologic consequences of discontinuing combination antiretroviral-drug therapy in HIV-infected patients with detectable viremia. *N. Engl. J. Med.* 344:472–480.
8. Finzi, D., M. Hermankova, T. Pierson, L. M. Carruth, C. Buck, R. E. Chaisson, T. C. Quinn, K. Chadwick, J. Margolick, R. Brookmeyer, J. Gallant, M. Markowitz, D. D. Ho, D. D. Richman, and R. F. Siliciano. 1997. Identification of a reservoir for HIV-1 in patients on highly active antiretroviral therapy. *Science* 278:1295–1300.
9. Finzi, D., J. Blankson, J. B. Margolick, K. Chadwick, T. Pierson, K. Smith, J. Lisziewicz, F. Lori, C. Flexner, T. C. Quinn, R. E. Chaisson, E. Rosenberg, B. Walker, S. Gange, J. Gallant, and R. F. Siliciano. 1999. Latent infection of CD4⁺ T cells provides a mechanism for lifelong persistence of HIV-1, even in patients on effective combination therapy. *Nat. Med.* 5:512–517.
10. Frost, S. D. W. 2001. Bayesian modeling of viral dynamics and evolution. *AIDS Cyber J.* 4(2). [Online.]
11. Furtado, M. R., D. S. Callaway, J. P. Phair, K. J. Kunstman, J. L. Stanton, C. A. Macken, A. S. Perelson, and S. M. Wolinsky. 1999. Persistence of HIV-1 transcription in peripheral-blood mononuclear cells in patients receiving potent antiretroviral therapy. *N. Engl. J. Med.* 340:1614–1622.
12. Garcia, F., M. Plana, C. Vidal, A. Cruceta, W. A. O'Brien, G. Pantaleo, T. Pumarola, T. Gallart, J. M. Miro, and J. M. Gatell. 1999. Dynamics of viral load rebound and immunological changes after stopping effective antiretroviral therapy. *AIDS* 13:F79–F86.
13. Garcia, F., M. Plana, G. M. Ortiz, S. Bonhoeffer, A. Soriano, C. Vidal, A. Cruceta, M. Arnedo, C. Gil, G. Pantaleo, T. Pumarola, T. Gallart, D. F. Nixon, J. M. Miro, and J. M. Gatell. 2001. The virological and immunological consequences of structured treatment interruptions in chronic HIV-1 infection. *AIDS* 15:F29–F40.
14. Gilks, W. R., S. Richardson, and D. J. Spiegelhalter (ed.). 1996. Markov Chain Monte Carlo in practice. Chapman & Hall, New York, N.Y.
15. Günthard, H. F., S. D. W. Frost, A. J. Leigh Brown, C. C. Ignacio, K. Kee, A. S. Perelson, C. A. Spina, D. V. Havlir, M. Hezareh, D. J. Looney, D. D. Richman, and J. K. Wong. 1999. Evolution of envelope sequences of HIV-1 in cellular reservoirs in the setting of potent antiviral therapy. *J. Virol.* 11:9404–9412.
16. Haslett, P. A. J., D. F. Nixon, Z. Shen, M. Larsson, W. I. Cox, R. Manandhar, S. M. Donahoe, and G. Kaplan. 2000. Strong human immunodeficiency virus (HIV)-specific CD4⁺-T-cell responses in a cohort of chronically infected patients are associated with interruptions in anti-HIV chemotherapy. *J. Infect. Dis.* 181:1264–1272.
17. Ho, D. D., A. U. Neumann, A. S. Perelson, W. Chen, J. M. Leonard, and M. Markowitz. 1995. Rapid turnover of plasma virions and CD4 lymphocytes in HIV-1 infection. *Nature* 373:123–126.
18. Hughes, J. P. 1999. Mixed effects models with censored data with application to HIV. *Biometrics* 55:625–629.
19. Imamichi, H., K. A. Crandall, V. Natarajan, M. K. Jiang, R. L. Dewar, S. Berg, A. Gaddam, M. Bosche, J. A. Metcalf, R. T. Davey, and H. C. Lane. 2001. Human immunodeficiency virus type 1 quaspecies that rebound after discontinuation of highly antiretroviral therapy are similar to the viral quaspecies present before initiation of therapy. *J. Infect. Dis.* 183:36–50.
20. Lifson, J. D., J. L. Rossio, R. Arnaout, L. Li, T. L. Parks, D. K. Schneider, R. F. Kiser, V. J. Coalter, G. Walsh, R. J. Imming, B. Fisher, B. M. Flynn, N. Bischofberger, M. Piatak, Jr., V. M. Hirsch, M. A. Nowak, and D. Wodarcz. 2000. Containment of simian immunodeficiency virus infection: cellular immune responses and protection from rechallenge following transient post-nucleation antiretroviral treatment. *J. Virol.* 74:2584–2593.
21. Lloyd, A. L. 2001. The dependence of viral parameter estimates on the assumed viral life cycle: limitations of studies of viral load data. *Proc. R. Soc. Lond. B* 268:847–854.
22. Lori, F., M. G. Lewis, J. Q. Xu, G. Varga, D. E. Zinn, C. Crabbs, W. Wagner, J. Greenhouse, P. Silvera, J. Yalley-Ogunro, C. Tinelli, and J. Lisziewicz. 2000. Control of SIV rebound through structured treatment interruptions during early infection. *Science* 290:1591–1593.
23. Lyles, R. H., C. M. Lyles, and D. J. Taylor. 2000. Random regression models for human immunodeficiency virus ribonucleic acid data subject to left censoring and informative drop-outs. *Appl. Stat.* 49:485–498.
24. Lynn, H. S. 2000. Maximum likelihood inference for left-censored HIV RNA data. *Stat. Med.* 20:33–45.
25. Masel, J., R. A. Arnaout, T. R. O'Brien, J. J. Goedert, and A. L. Lloyd. 2000. Fluctuations in HIV-1 viral load are correlated to CD4⁺-T-lymphocyte count

- during the natural course of infection. *J. Acquir. Immune Defic. Syndr.* **23**:375–379.
26. **Miller, V.** 2001. Structured treatment interruptions in antiretroviral management of HIV-1. *Curr. Opin. Infect. Dis.* **14**:29–37.
 27. **Mollet, L., T. S. Li, A. Samri, C. Tournay, R. Tubiana, V. Calvez, P. Debre, C. Katlama, and B. Autran.** 2000. Dynamics of HIV-specific CD8⁺ T lymphocytes with changes in viral load. *J. Immunol.* **165**:1692–1704.
 28. **Neumann, A. U., R. Tubiana, V. Calvez, C. Robert, T. S. Li, H. Agut, and B. Autran.** 1999. HIV-1 rebound during interruption of highly active antiretroviral therapy has no deleterious effect on reinitiated treatment. *AIDS* **13**: 677–683.
 29. **Nowak, M. A., and C. R. M. Bangham.** 1996. Population dynamics of immune response to persistent viruses. *Science* **272**:74–79.
 30. **Nowak, M. A., A. L. Lloyd, G. M. Vasquez, T. A. Wiltrout, L. M. Wahl, N. Bischoffberger, J. Williams, A. Kinter, A. S. Fauci, V. M. Hirsch, and J. D. Lifson.** 1997. Viral dynamics of primary viremia and antiretroviral therapy in simian immunodeficiency virus infection. *J. Virol.* **71**:7518–7525.
 31. **Ortiz, G. M., D. F. Nixon, A. Trkola, J. Binley, X. Jin, S. Bonhoeffer, P. J. Kuebler, S. M. Donahoe, M. A. Demoitie, W. M. Kakimoto, T. Ketas, B. Clas, J. J. Heymann, L. Q. Zhang, Y. Z. Cao, A. Hurley, J. P. Moore, D. D. Ho, and M. Markowitz.** 1999. HIV-1-specific immune responses in subjects who temporarily contain virus replication after discontinuation of highly active antiretroviral therapy. *J. Clin. Investig.* **104**:R13–R18.
 32. **Papasavvas, E., G. M. Ortiz, R. Gross, J. W. Sun, E. C. Moore, J. J. Heymann, M. Moonis, J. K. Sandberg, L. A. Drohan, B. Gallagher, J. Shull, D. F. Dixon, J. R. Kostman, and L. J. Montaner.** 2000. Enhancement of human immunodeficiency virus type 1-specific CD4 and CD8 T-cell responses in chronically infected persons after temporary treatment interruption. *J. Infect. Dis.* **182**:766–775.
 33. **Perelson, A. S., A. U. Neumann, M. Markowitz, J. M. Leonard, and D. D. Ho.** 1996. HIV-1 dynamics in vivo: virion clearance rate, infected cell life-span, and viral generation time. *Science* **271**:1582–1586.
 34. **Perelson, A. S., P. Essunger, Y. Z. Cao, M. Vesanan, A. Hurley, K. Saksela, M. Markowitz, and D. D. Ho.** 1997. Decay characteristics of HIV-1 infected compartments during combination therapy. *Nature* **387**:188–191.
 35. **Pinheiro, J. C., and D. M. Bates.** 2000. *Mixed-effects models in S and S-PLUS.* Springer-Verlag, New York, N.Y.
 36. **Plummer, M., N. G. Best, K. Cowles, and K. Vines.** 2000. CODA: output analysis and diagnostics for MCMC. MRC Biostatistics Unit, Cambridge, United Kingdom. [Online.]
 37. **Rosenberg, E. S., M. Altfeld, S. H. Poon, M. N. Phillips, B. M. Wilkes, R. L. Eldridge, G. K. Robbins, R. T. D'Aquila, P. J. R. Goulder, and B. D. Walker.** 2000. Immune control of HIV-1 after early treatment of acute infection. *Nature* **407**:523–526.
 38. **Ruiz, L., J. Martinez-Picado, J. Romeu, R. Paredes, M. K. Zayat, S. Marfil, E. Negro, G. Sirera, C. Tural, and B. Clotet.** 2000. Structured treatment interruption in chronically HIV-1 infected patients after long-term viral suppression. *AIDS* **14**:397–403.
 39. **Ruiz, L., G. Carcelain, J. Martinez-Picado, S. Frost, S. Marfil, R. Paredes, J. Romeu, E. Ferrer, K. Morales-Lopez, M. K. Zayat, B. Autran, and B. Clotet.** 2001. HIV-specific CD8⁺ T cells and HIV dynamics after three structured treatment interruptions in chronic HIV infection. *AIDS* **15**:F19–F27.
 40. **Schuurman, R., D. Descamps, G. J. Weverling, S. Kaye, J. Tijnagel, I. Williams, R. van Leeuwen, R. Tedder, C. A. B. Boucher, F. Brun Vezinet, and C. Loveday.** 1996. Multicenter comparison of three commercial methods for quantification of human immunodeficiency virus type 1 RNA in plasma. *J. Clin. Microbiol.* **34**:3016–3022.
 41. **Smith, B. A., S. Gartner, Y. Liu, A. S. Perelson, N. I. Stilianakis, B. F. Keele, T. M. Kerker, A. Ferreira-Gonzalez, A. K. Szakal, J. G. Tew, and G. F. Burton.** 2001. Persistence of infectious HIV on follicular dendritic cells. *J. Immunol.* **166**:690–696.
 42. **Spiegelhalter, D. J., A. Thomas, and N. G. Best.** 2000. WinBUGS version 1.2 user manual. MRC Biostatistics Unit, Cambridge, United Kingdom. [Online.]
 43. **Wand, M. P., and M. C. Jones.** 1995. *Kernel smoothing.* Chapman and Hall, New York, N.Y.
 44. **Wei, X., S. Ghosh, M. E. Taylor, V. A. Johnson, E. A. Emini, P. Deutsch, J. D. Lifson, S. Bonhoeffer, M. A. Nowak, B. H. Hahn, M. S. Saag, and G. M. Shaw.** 1995. Viral dynamics in human immunodeficiency virus type 1 infection. *Nature* **373**:117–122.
 45. **Wodarz, D., and M. A. Nowak.** 1999. Specific therapy regimes could lead to long-term immunological control of HIV. *Proc. Natl. Acad. Sci. USA* **96**: 14464–14469.
 46. **Wodarz, D., R. A. Arnaout, M. A. Nowak, and J. D. Lifson.** 2000. Transient antiretroviral treatment during acute simian immunodeficiency virus infection facilitates long-term control of the virus. *Phil. Trans. R. Soc. Lond. B* **355**:1021–1029.
 47. **Wong, J. K., M. Hezareh, H. F. Günthard, D. V. Havlir, C. C. Ignacio, C. A. Spina, and D. D. Richman.** 1997. Recovery of replication-competent HIV despite prolonged suppression of plasma viremia. *Science* **278**:1291–1295.
 48. **Zhang, L., B. Ramratnam, K. Tenner-Racz, Y. X. He, M. Vesanan, S. Lewin, A. Talal, P. Racz, A. S. Perelson, B. T. Korber, M. Markowitz, and D. D. Ho.** 1999. Quantifying residual HIV-1 replication in patients receiving combination antiretroviral therapy. *N. Engl. J. Med.* **340**:1605–1613.
 49. **Zhang, L. Q., C. Chung, B. S. Hu, T. He, Y. Guo, A. J. Kim, E. Skulsky, X. Jin, A. Hurley, B. Ramratnam, M. Markowitz, and D. D. Ho.** 2000. Genetic characterization of rebounding HIV-1 after cessation of highly active antiretroviral therapy. *J. Clin. Investig.* **106**:839–845.